

# The mechanism of oxidation of 3-mercaptopropionic acid

Paula Forlano, José A. Olabe, Jorge F. Magallanes, and Miguel A. Blesa

**Abstract:** The mechanism of the oxidation of 3-mercaptopropionic acid (3-MPA) by hydrogen peroxide was studied in the acidic pH range. The nucleophilic attack by sulphur on the peroxide bond controls the rate. Extrapolation of the pH dependency suggests that the rate of attack by the deprotonated dianion is highest. Traces of Fe(III), at levels below  $10^{-7}$  mol dm $^{-3}$ , do not catalyze efficiently the process through one-electron mechanisms; at higher concentrations, or on the surface of iron(III) oxides, this type of catalysis becomes important. The electrochemical oxidation of 3-MPA was also studied, using differential pulse polarography and cyclic voltammetry techniques. The mechanism is of the EC $_2$ E type, the second electron transfer step corresponding to the oxidation of the disulphide RS-SR. The rate constant for the dimerization of the RS $^{\bullet}$  radicals was  $1.8 \times 10^3$  mol $^{-1}$  dm $^3$  s $^{-1}$ ; the slowness of this step agrees with the mechanisms observed in the course of one-electron oxidations by metal ions.

**Key words:** electrochemistry, kinetics, 3-mercaptopropionic acid, autooxidation.

**Résumé :** Opérant dans la plage acide des pH, on a étudié le mécanisme d'oxydation de l'acide 3-mercaptopropanoïque («3-MPA») par le peroxyde d'hydrogène. La vitesse de la réaction est fixée par l'attaque nucléophile du soufre sur la liaison peroxyde. Une extrapolation de la dépendance sur le pH suggère que l'attaque par le dianion déprotoné est celle qui se fait avec la vitesse la plus grande. Le fer(III), à l'état de traces, à des niveaux inférieurs à  $10^{-7}$  mol dm $^{-3}$ , ne catalyse pas le processus d'une façon efficace par le biais de mécanismes à un électron; à des concentrations plus élevées, ou sur la surface d'oxydes de fer(III), ce type de catalyse devient important. On a aussi examiné l'oxydation électrochimique du «3-MPA» en faisant appel à des techniques de polarographie différentielle pulsée et de voltampérométrie cyclique. Le mécanisme de cette réaction est du type EC $_2$ E, l'étape du deuxième transfert d'électron correspondant à l'oxydation du disulfure RS-SR. La constante de vitesse de dimérisation des radicaux RS $^{\bullet}$  est égale à  $1,8 \times 10^3$  mol $^{-1}$  dm $^3$  s $^{-1}$ ; la lenteur de cette étape est en accord avec les mécanismes observés lors des oxydations à un électron en présence d'ions métalliques.

**Mots clés :** électrochimie, cinétique, acide 3-mercaptopropanoïque, autooxydation.

[Traduit par la rédaction]

## Introduction

The oxidation of mercaptocarboxylic acids is a reaction of importance in biological systems, and has therefore been studied by several authors (1–7). The oxidation of other organic compounds, such as thiourea or thiols, has also been the subject of extensive research (8–11). It seems clear that no single

mechanism is involved in all cases, although the disulphide is generally the main "initial" product. The formation of disulphide may be mediated by sulphenic acids R-SOH originating in the attack of hydrogen peroxide on the deprotonated R-S $^-$  moiety, or by R-S $^{\bullet}$  free radicals formed by attack of OH $^{\bullet}$  on R-S(H $^+$ ), the OH $^{\bullet}$  radical having been formed by radiolysis, or by chemical means from H $_2$ O $_2$  (metal ion catalysis).

The present note reports a study of the oxidation of 3-mercaptopropionic acid both by hydrogen peroxide and in an electrochemical cell. In the former case, the influence of added Fe(III) was cursorily explored to define the limits of relevance of direct attack and radical, Fenton-like mechanisms. The intervention of these latter mechanisms was also explored in heterogeneous media, i.e., under conditions of iron oxide catalyzed H $_2$ O $_2$  decomposition.

## Experimental

All reagents were analytical grade; tridistilled water was used to prepare the solutions, the last two distillations being made in a quartz apparatus. Hydrogen peroxide free of stabilizers was used as solutions freshly prepared and titrated against a KMnO $_4$  standard solution. Fe(III) stock solution was prepared by oxidation with H $_2$ O $_2$  of a Fe(II) solution obtained by dissolving the metal in HClO $_4$  and titrated potentiometrically against standard K $_2$ Cr $_2$ O $_7$ .

Received March 29, 1996.<sup>1</sup>

**P. Forlano and J.A. Olabe.** Instituto de Química Física de Materiales, Medio Ambiente y Energía (INQUIMAE), Departamento de Química Inorgánica, Analítica y Química Física, Facultad de Ciencias Exactas y Naturales, Universidad de Buenos Aires, Ciudad Universitaria, Pabellón II, 1428 Buenos Aires, Argentina.

**J.F. Magallanes and M.A. Blesa.**<sup>2</sup> Instituto de Química Física de Materiales, Medio Ambiente y Energía (INQUIMAE), Departamento de Química Inorgánica, Analítica y Química Física, Facultad de Ciencias Exactas y Naturales, Universidad de Buenos Aires, Ciudad Universitaria, Pabellón II, 1428 Buenos Aires, Argentina, and Unidad de Actividad Química, Comisión Nacional de Energía Atómica, Avenida del Libertador 8250, 1429 Buenos Aires, Argentina.

<sup>1</sup> Revision received November 4, 1996.

<sup>2</sup> Author to whom correspondence may be addressed.  
Telephone: (54-1) 704-1367. Fax: (54-1)-704-1164.  
E-mail: miblesa@cnea.edu.ar

The ionic strength was kept constant at  $4 \times 10^{-3}$  M using  $\text{HClO}_4$  and  $\text{NaClO}_4$  solutions. This ionic strength was high enough to ensure appropriate behavior of the differential pulse polarography (dpp) waves in the experiments described below. The reversibility of 3-MPA oxidation was checked, and the width at half-peak height ( $W_{1/2}$ ) of dpp was found to agree with the theoretical values of the Heijne and Van der Linden (12) treatment, over the whole 3-MPA concentration range explored ( $4 \times 10^{-5}$  –  $4 \times 10^{-4}$  M).

### Oxidation by hydrogen peroxide

The kinetics of the oxidation of 3-MPA by  $\text{H}_2\text{O}_2$  was studied in the pH range 2.4–6. The decrease of the 3-MPA peak height during oxidation was followed by measuring the height of the dpp wave. The concentration was obtained from the linear calibration plot (peak height vs. concentration) previously determined for each pH value. Solutions of  $10^{-4}$  M 3-MPA were prepared and the pH adjusted with  $\text{HClO}_4$ . The solution was placed in the thermostatted (25°C) cell of a PAR 174A polarographic analyzer, with a dropping or hanging drop Hg electrode, a Pt wire auxiliary electrode, and the reference electrode. All potentials were measured against a Ag/AgCl, KCl saturated reference electrode. Differential pulse polarograms (dpp) were obtained at  $t = 0$  and sequentially after the addition of the adequate amount of hydrogen peroxide; all experiments were conducted under conditions of excess  $\text{H}_2\text{O}_2$ . The 3-MPA oxidation wave is found in the range between  $-0.35$  and  $0.40$  V, with  $E_{1/2} = -0.15$  V. At concentrations higher than  $7 \times 10^{-4}$  mol  $\text{dm}^{-3}$ , a new wave appears at more positive potentials, due to multilayer formation on the adsorbed monolayer (13). The reaction is slow enough to permit the sequential determination of 3-MPA. Occasionally, hydrogen peroxide was determined using its reduction wave in the range  $-0.35$  to  $-1.85$  V ( $E_{1/2} = -0.96$  V) (14).

To assess the possible operation of metal ion catalysis, measurements were also carried out in the presence of EDTA, or in the presence of added iron(III) perchlorate, in the concentration range  $10^{-8}$ – $10^{-6}$  mol  $\text{dm}^{-3}$ .

### Electrochemical oxidation

The mechanism of the electrochemical oxidation was explored by using polarographic and cyclic voltammetric (CV) techniques at pH = 2.4. The dependence of  $E_{1/2}$  on the 3-MPA concentration and the  $W_{1/2}$  of differential pulse polarography was measured. Experiments were also carried out at different drop times.

A complementary set of CV experiments were done at sweep rates between 10 and 200  $\text{mV s}^{-1}$  and various 3-MPA concentrations. In the range  $3 \times 10^{-4}$  –  $5 \times 10^{-3}$  mol  $\text{dm}^{-3}$  of 3-MPA, no multilayer effect is observed.

## Results and discussion

### Oxidation by hydrogen peroxide

At constant pH and  $[\text{H}_2\text{O}_2]$ , plots of  $\ln([\text{MPA}]/[\text{MPA}]_0)$  vs. time yield straight lines from which pseudo-first-order rate constants can be obtained. Figure 1 shows the plot of the pseudo-first-order constants at pH = 2.4 as a function of  $[\text{H}_2\text{O}_2]$ , which demonstrates that the kinetic law is

$$[1] \quad R = k[\text{MPA}][\text{H}_2\text{O}_2]$$

Fig. 1. Dependence of the pseudo-first-order rate constants upon  $[\text{H}_2\text{O}_2]$  at pH = 2.4 and 298 K, ionic strength  $4 \times 10^{-3}$  M.

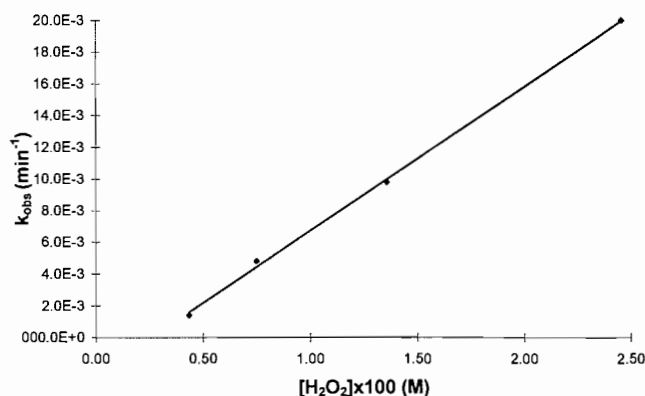
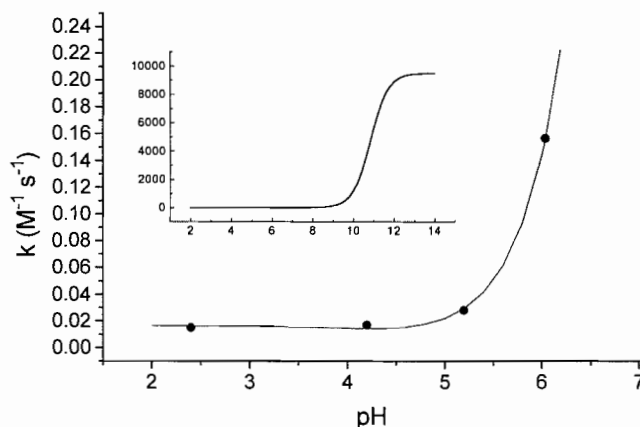


Fig. 2. pH dependence of the second-order rate constant for the reaction of 3-MPA upon  $\text{H}_2\text{O}_2$  at 298 K, ionic strength  $4 \times 10^{-3}$  M: (●) experimental points; (—) eq. [2]. Inset: pH dependence of the empirical rate constant  $k$  (eq. [1]) according to eq. [2].



where  $[\text{MPA}]$  represents the total (analytical) concentration of 3-mercaptopropionic acid.

The straight line in Fig. 1 extrapolates to an apparent negative rate for  $[\text{H}_2\text{O}_2] = 0$ ; this behavior is most probably an experimental artifact associated with some decomposition of hydrogen peroxide.

Figure 2 shows the pH dependency of  $k$ , together with the curve drawn assuming that the general eq. [2] can be used to describe the pH effects in terms of the contribution of three parallel pathways to eq. [1], each path corresponding to the reaction with hydrogen peroxide of each of the three protolysis species of 3-MPA. The values  $\text{p}K_{a1} = 4.34$  and  $\text{p}K_{a2} = 10.84$  (taken from ref. 15) were used to calculate the concentration of each species at each pH.

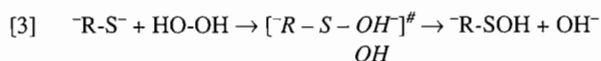
$$[2] \quad k = (k_1[\text{H}_2\text{X}] + k_2[\text{HX}^-] + k_3[\text{X}^{2-}]) / [\text{MPA}]$$

where  $\text{X}^{2-}$  represents the dianion of 3-MPA.

The data were collected in a pH range well below  $\text{p}K_{a2}$  and the steep rise in rate at the highest pH explored can be accounted for only if it is assumed that the reactivity is essentially governed by the dianion. From our data, it is not possible to derive a value for  $k_2$ ; only an upper limit can be given. The

second-order rate constants that yield the best fit shown in Fig. 2 are (in  $\text{mol}^{-1} \text{dm}^3 \text{s}^{-1}$ )  $k_1 = 1.6 \times 10^{-2}$ ;  $k_2 = 10^{-2}$ ;  $k_3 = 9.5 \times 10^3$ .

This kinetic law is compatible with a rate-determining direct attack by sulphur on hydrogen peroxide, the rate being highest for the deprotonated sulphur of the dianion:



This mechanism involves a nucleophilic attack on hydrogen peroxide. The ensuing population of the LUMO of  $\text{H}_2\text{O}_2$  (mainly antibonding about the peroxide bond) results in O—O bond breaking. The simplest stoichiometry of the reaction results from the further fast reaction of the sulphenic derivative RSOH with RSH:



but other products may also form in the presence of excess oxidant (7, 16).

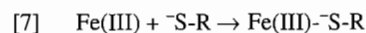
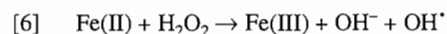
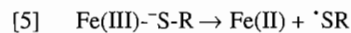
Barton et al. (3) have studied the analogous reactions of cysteine and cysteamine, and report second-order rate constants of 12.4 and  $10 \text{ mol}^{-1} \text{dm}^3 \text{s}^{-1}$  for the corresponding zwitterionic species,  $^+\text{H}_3\text{N-R-S}^-$ . These two values are strikingly similar, taking into account that cysteine bears a net negative charge due to the ionized carboxylate group. It is also reported that the corresponding anions  $\text{H}_2\text{N-R-S}^-$  react more slowly. Of particular interest is the comparison of cysteine (2-amino-3-mercaptopropionic acid) and 3-MPA. The dianion  $^-\text{O}_2\text{CCH}_2\text{CH}_2\text{S}^-$  is more basic than  $^-\text{O}_2\text{CCH}(\text{NH}_2)\text{CH}_2\text{S}^-$  (the corresponding  $\text{pK}_a$  values of the conjugate acids are 10.84 and 8.53, respectively). The former dianion is also more reactive towards  $\text{H}_2\text{O}_2$ , and 3-MPA reacts faster at any given pH value (correspondingly, the pH range spanned in our study is lower than that explored by Barton et al. (3)). The presence of the amino group in the 2-position is seen to affect profoundly the basicity of the  $\text{R-S}^-$  group. The decrease in basicity is related to the very large decrease in the rate of attack on the peroxide bond. In agreement, in a separate study, we have found that the rates of coordination through sulphur to  $[\text{Ru}^{\text{III}}(\text{edta})\text{H}_2\text{O}]^-$  by various  $\text{R-SH}$  ligands correlate with the  $\text{pK}_a$  values of the  $-\text{SH}$  group.<sup>3</sup> Also in agreement, we have shown previously that the rate of reductive attack on iron(III) oxides by 3-MPA is much larger than that of cysteine (17). An important consequence is that the amino group gives some protection to cysteine against hydrogen peroxide attack at physiological pH.

Protonation of the leaving OH group of hydrogen peroxide at low pH catalyzes the attack of thiourea on  $\text{H}_2\text{O}_2$  (8); a related phenomenon has been involved in the reaction of the cysteine zwitterion, even though the bulk pH in this case precludes equilibrium protonation of  $\text{H}_2\text{O}_2$ . Acid catalysis is totally ruled out under our experimental conditions. The very small effect of the carboxylate group, as documented by the comparison of cysteine and cysteamine, still remains unexplained.

### The influence of Fe(III)

It is well known that Fe(III) oxidizes mercaptocarboxylic acids to disulphides, through an inner-sphere reaction (4). This reaction takes place both with dissolved Fe(III) salts and with suspended iron(III) oxides (17) (in this case, the anaerobic oxidation of 3-MPA by Fe(III) takes place along with oxide dissolution). In the heterogeneous case, addition of excess hydrogen peroxide shifts the stoichiometry of the reaction to the catalyzed oxidation of 3-MPA, with negligible dissolution.

The coupling of the internal redox decomposition of Fe(III)-mercaptocarboxylate complexes and the reoxidation of Fe(II) by hydrogen peroxide may lead to the catalytic oxidation of mercaptocarboxylic acids:

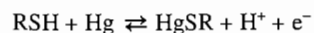


The reaction scheme is completed with the fast scavenging of  $\text{OH}^\cdot$  by HSR.

The possible contribution of free radicals due to Fenton-type reactions of hydrogen peroxide with metal ion impurities was explored in a series of experiments with added EDTA and added Fe(III). In the presence of EDTA, the measured rates were identical to those discussed above. Added Fe(III), on the other hand, led to erratic rate changes; for example, a fivefold rate enhancement was observed when  $[\text{Fe(III)}] = 10^{-7} \text{ mol dm}^{-3}$ . Although the rate generally increased upon addition of Fe(III), no clear relationship could be observed between the rates and  $[\text{Fe(III)}]$ . Although this reaction pathway may become important under adequate experimental conditions, at pH 2.4 the stability of the complex and rates of internal redox decomposition are low enough to make the rate of the catalyzed reaction (at  $[\text{Fe(III)}]$  below  $10^{-7} \text{ mol dm}^{-3}$ ) slow in comparison with the direct bimolecular reaction. The rate values reported above are therefore not affected by contributions of this type.

### Electrochemical oxidation

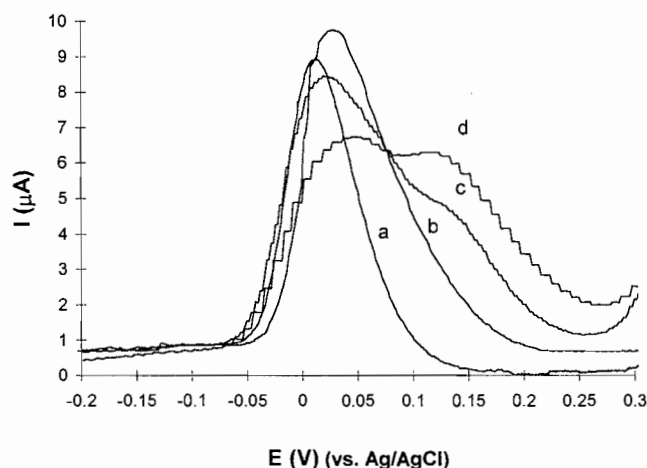
As early as 1940 Kolthoff, Barnum, and Lingane (18, 19, and refs. therein) studied the polarographic anodic oxidation of cysteine. They found that the reaction is not reversible, even in 0.1 M  $\text{HClO}_4$ . At higher pH ( $> 2$ ) abnormal waves are obtained because of the strong adsorption on the mercury electrode. At low concentration (0.002 M) the reaction is diffusion controlled, but at higher concentration the film formation controls the current. After considering several possible mechanisms, including the  $\text{EC}_2$  (EDIM), these authors conclude that the reaction mechanism is simply



The dimerization stage of  $\text{RS}^\cdot$  radicals to yield the disulphide is therefore inhibited by the stability of adsorbed  $\text{Hg(I)}$  salt. Birke and Mazorra report that  $\text{Hg(SR)}_2$  layers may be formed in the oxidation of several thiols. Our results in the oxidation of 3-mercaptopropionic acid at pH 2.4 bear some similarities, but there is clear evidence for an  $\text{EC}_2\text{E}$  (EDIME) mechanism, in which the disulphide  $\text{RS-SR}$  is involved, as discussed below.

<sup>3</sup> V. Povse and J.A. Olabe. Work in progress.

**Fig. 3.** The dpp traces of the oxidation of 3-MPA at pH = 2.4 for various drop times. (a): 0.5 s, (b): 1 s, (c): 2 s, (d): 5 s.

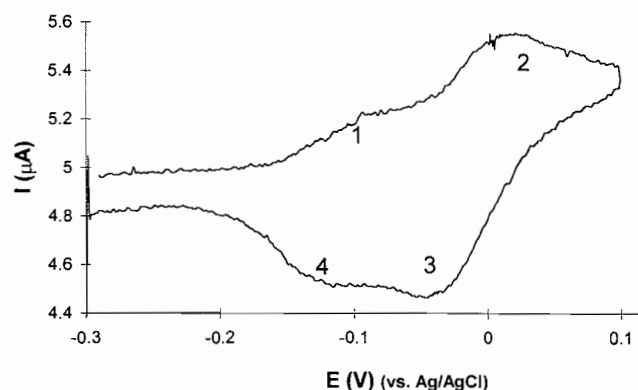


The dpp of 3-MPA in  $4 \times 10^{-3}$  mol dm $^{-3}$  HClO $_4$  shows a value of  $W_{1/2} = 80.5$  mV, appreciably lower than the theoretical value for reversible one-electron transfer, 92.8 mV (12). This observation suggests that more than one electron is transferred in the overall reaction.

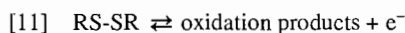
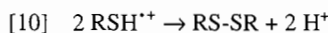
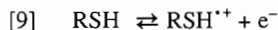
When the 3-MPA concentration is increased, the maximum of the dpp oxidation wave  $E_p$  shifts to more negative potentials. As  $E_p = E_{1/2} + \Delta E/2$  (where  $\Delta E$  is the modulation potential) the shift in  $E_p$  with concentration is identical with the shift in  $E_{1/2}$ , and the observed behavior is indicative of an EC-type mechanism (20), at variance with the mechanism postulated by Kolthoff and Barnum for cysteine. The plot of  $E_{1/2}$  vs.  $\ln [\text{MPA}]$  is linear, the slope being 13.3 mV/decade. This value is identical within the error limits with the theoretical slope for an EC $_2$  (EDIM) mechanism involving one-electron transfer and surface reaction of adsorbed species,  $RT/2nF = 12.85$  mV at 25°C (20). For an EDIM mechanism involving a "volume" reaction (no adsorption), Mairanovskii (20) and Koutecky and Hanus (22) found that this slope is  $RT/3nF = 8.5$  mV.

Figure 3 shows a set of dpp traces at different drop times. At short drop times, a single wave is observed; when the drop time increases, a second wave at more positive potentials emerges progressively. For a modulation potential of 25 mV and drop time 1 s, the difference between the potentials of both waves is 28 mV; separate experiments with pure disulphide demonstrated that the dpp oxidation wave of this compound reaches the maximum at a potential positively shifted from the value for 3-MPA by 22.2 mV. In view of the different experimental conditions (no adsorbed reactant, no overlapped waves), the agreement is reasonably good, and it may be concluded that the second wave observed in Fig. 3 is due to the oxidation of RS-SR. This process may be observed only when the drop time is long enough to permit dimer formation, and an EC $_2$ E mechanism is thus suggested, involving a second electron transfer stage that produces reversibly an otherwise undefined oxidation product. No experimental evidence on the nature of this product is available. Several experimental characteristics of the disulphide oxidation indicate a one-electron reaction. In CV experiments (Fig. 4, peaks 2 and 3), the  $\Delta E_{\text{peak}}$  (anodic – cathodic) is 63 mV; also, the peak position does not

**Fig. 4.** Voltammogram of 3-MPA at pH 2.4, scan rate 100 mV s $^{-1}$ . Peaks 1 and 2 correspond to reaction steps [9] and [11], respectively (see text).



shift with the sweep rate. Finally, in dpp,  $W_{1/2} = 94$  mV indicates a reversible one-electron transfer. This mechanism also accounts for the small difference between the theoretical and the calculated slope in the  $E_{1/2}$  vs.  $\ln [\text{MPA}]$  plots:



The voltammograms of 3-MPA show four peaks, corresponding to the two electron transfers, the intensity and position of which are dependent on sweep rate. Figure 4 shows an example; although the definition of some peaks was poor (for instance peaks 1 and 4 in Fig. 4), it was possible to draw clear conclusions from the analysis of the whole set of voltammograms. In particular, the ratio of the heights of peaks 2 and 4 is strongly dependent on the sweep rate:  $I_{p2}/I_{p4}$  decreases when the sweep rate increases, as expected for the above mechanism. From the values of  $I_{p2}/I_{p4}$  for various 3-MPA concentrations, measured at two sweep rate values,  $v = 50$  and 100 mV s $^{-1}$ , the value of the radical dimerization (eq. [10]) rate constant  $k_{\text{dim}}$  may be calculated. The calculations must be done by simulation of the  $I_{p2}/I_{p4}$  ratio as a function of the dimensionless rate constant  $k_{\text{sim}}$ , defined by eqs. [12] and [13]:

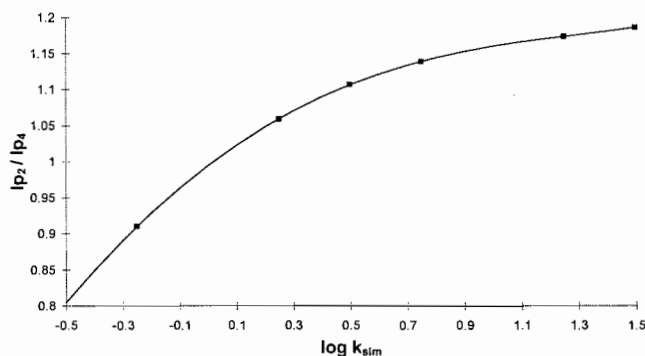
$$[12] \quad k_{\text{sim}} = k_{\text{dim}}([\text{MPA}]/a)$$

where:

$$[13] \quad a = nFv/RT$$

An explicit digital simulation, based on the exponential expanded space grid method developed by S.W. Feldberg (23) was used. Details of this program applied to a similar mechanism are explained in ref. 24. Due to the overlapping of  $I_{p1}/I_{p2}$  and  $I_{p3}/I_{p4}$ , the ratio would be difficult to measure using the basic analytical theories of voltammetry. However, because the separation between  $E_{1/2}$  for reactions [9] and [11] is measured experimentally, the digital simulation of the system leads to a set of partially overlapped waves, similar to those

**Fig. 5.** Simulated  $I_{p2}/I_{p4}$  ratio as a function of  $\log k_{sim}$  (see text for further details).



obtained in practice. The simulated and experimental  $I_{p2}/I_{p4}$  ratios behave similarly.

Figure 5 shows the simulated function  $I_{p2}/I_{p4} = f(\log k_{sim})$ ; interpolation of the experimental  $I_{p2}/I_{p4}$  values yields values of  $k_{sim}$  from which  $k_{dim}$  may be obtained, using eq. [12]. The dependence of  $k_{sim}$  on the concentration at constant sweep rates is indeed linear, and from the slopes at  $v = 50$  and  $100 \text{ mV s}^{-1}$ , the derived values of  $k_{dim}$  are  $1.7(\pm 0.2) \times 10^3$  and  $1.97(\pm 0.04) \times 10^3 \text{ mol dm}^{-3} \text{ s}^{-1}$ .

As a further check, simulated voltammograms were computed using these  $k_{dim}$  values; a reasonable coincidence between simulated and experimental traces was obtained. Also, the relative heights of the dpp waves at different drop times can be calculated using  $k_{dim}$  to estimate the concentration of 3-MPA on the electrode surface. For drop times of 2 and 5 s, the height ratio is calculated to be 0.74, as compared with an experimental ratio of 0.83. The lack of data at other drop times precludes further elaboration of this point.

The slowness of radical dimerization poses a certain limitation to the operation of one-electron chemical oxidation of 3-MPA, because the reverse regeneration of the dianion may become important. In fact, in the course of oxidation by one-electron metallic oxidants such as Fe(III), the activated complex composition normally reflects the need to bring together two oxidants, thus allowing the formation of the disulphide in a more efficient way (17). In view of the large atom transfer rate constant between the dianion of 3-MPA and hydrogen peroxide, it is not surprising that the radical pathway does not contribute significantly to the reaction mechanism.

## Acknowledgments

This work was partially supported by grants from the Univer-

sity of Buenos Aires and Fundación Antorchas. J.A.O. and M.A.B. are members of the National Research Council (CONICET).

## References

1. R.G. Neville. *J. Am. Chem. Soc.* **79**, 2456 (1957).
2. I. Pascal and D.S. Tarbell. *J. Amer. Chem. Soc.* **79**, 6015 (1957).
3. J.P. Barton, J.E. Packer, and R.J. Sims. *J. Chem. Soc. Perkin Trans. 2*, 1547 (1973).
4. C. Baiocchi, E. Mentasti, and P. Arselli. *Transition Met. Chem. (London)*, **8**, 40 (1983), and refs. therein.
5. R.F. Jameson, W. Linert, A. Tschinkowitz, and V. Gutmann. *J. Chem. Soc. Dalton Trans.* 943 (1988) (correction on p. 2243 (1988)).
6. R.F. Jameson, W. Linert, and A. Tschinkowitz. *J. Chem. Soc. Dalton Trans.* 2109 (1988).
7. E. Deutsch, M.J. Root, and D.L. Nosco. *Adv. Inorg. Bioinorg. Mech.* 269 (1983).
8. R.M. Hoffmann and J.O. Edwards. *Inorg. Chem.* **16**, 3333 (1977).
9. K. Leung and M.R. Hoffmann. *J. Phys. Chem.* **89**, 5267 (1985).
10. K. Leung and M.R. Hoffmann. *J. Phys. Chem.* **93**, 431 (1989).
11. M.R. Hoffmann. *In Aquatic chemical kinetics. Edited by W. Stumm.* Wiley, New York. 1990. pp. 71–111.
12. G.J.M. Heijne and W.E. Van der Linden. *Anal. Chim. Acta*, **82**, 231 (1976).
13. R.L. Birke and M. Mazorra. *Anal. Chim. Acta*, **118**, 257 (1980).
14. I.M. Kolthoff and J.J. Lingane. *In Polarography. Vol. 2.* Interscience Publishers, New York. 1952. pp. 552–553.
15. E.A. Martell and R.M. Smith. *In Critical stability constants. Vol. 1.* Plenum Press, New York. 1974.
16. F.A. Davis and R.L. Billmers. *J. Am. Chem. Soc.* **103**, 7016 (1981).
17. E.B. Borghi, P.J. Morando, and M.A. Blesa. *Langmuir*, **7**, 1652 (1991).
18. I.M. Kolthoff and C. Barnum. *J. Am. Chem. Soc.* **62**, 3061 (1940).
19. I.M. Kolthoff and J.J. Lingane. *In Polarography. Vol. 2.* Interscience Publishers, New York. 1952. pp. 781–791.
20. S.G. Mairanovskii. *In Catalytic and kinetic waves in polarography.* Plenum Press, New York. 1968. pp. 228–231.
21. E. Laviron and R. Meunier-Prest. *J. Electroanal. Chem.* **375**, 79 (1994).
22. J. Koutecky and V. Hanus. *Collect. Czech. Chem. Commun.* **28**, 446 (1970).
23. S.W. Feldberg. *J. Electroanal. Chem.* **127**, 1 (1981).
24. J.M. Marioli, J.F. Magallanes, and L. Sereno. *Bol. Soc. Chil. Quim.* **36**, 157 (1991).